

# Toughening and Strengthening of Alumina with Silver Inclusions

W. B. Chou & W. H. Tuan\*

Institute of Materials Science & Engineering, National Taiwan University, Taipei, Taiwan 10764

(Received 23 June 1993; received in revised form 20 June 1994; accepted 27 June 1994)

## Abstract

The fracture toughness and flexural strength of  $Al_2O_3/Ag$  composites are investigated. Both the strength and toughness of alumina are enhanced as silver inclusions are added. From microstructural observation, the crack is bridged or deflected by silver inclusions. The toughness enhancement is contributed mainly by the plastic deformation of the silver inclusions. The strengthening effect is contributed both by the matrix grain refinement and by the toughness enhancement.

## 1 Introduction

The application of ceramics as structural components is often limited by their brittleness. A major research objective has therefore been to improve their toughness. Previous studies have demonstrated that brittle solids can be toughened by incorporating metallic inclusions into them.<sup>1–7</sup> Similar to the zirconia toughened ceramics (ZTC),<sup>8</sup> the toughness of the metal-toughened ceramics can be described as

$$K_{IC, composite} = K_{IC, matrix} + \Delta K_{IC, metal} \quad (1)$$

where  $K_{IC, composite}$  is the toughness of the composite,  $K_{IC, matrix}$  the toughness of the matrix and,  $\Delta K_{IC, metal}$  the toughness increase contributed by the metallic reinforcement. The toughness enhancement for the ceramic–metal composites is believed to be contributed by the plastic deformation of metallic inclusions.<sup>9–11</sup>

As metallic inclusions are embedded within ceramic matrices, the metallic inclusion is constrained by the brittle and rigid matrix. The deformation behaviour of the constrained inclusion has been investigated by Ashby *et al.*<sup>9–10</sup> They suggested that the toughness increase, contributed by plastic deformation,  $\Delta K_{IC, plastic deformation}$  is propor-

tional to square root of the product of the volume fraction,  $F$ , and the inclusion size,  $d$ , as

$$\Delta K_{IC, plastic deformation} = C (F d)^{1/2} \quad (2)$$

where  $C$  is a constant. The constant depends on the bonding characteristics. Deve *et al.* have suggested that the toughness enhancement is increased with the increase of the ductility of metallic inclusion.<sup>11</sup> Among metals, silver is superior for its ductility. Furthermore, silver is chemically stable up to temperatures higher than its melting point, 960°C. Therefore, the silver containing composites can be prepared by pressureless sintering in air.<sup>12,13</sup>

The mechanical properties of  $Al_2O_3/Ag$  composites have been studied recently.<sup>12,13</sup> In these studies, the toughness is determined by the indentation technique. As we are going to show later, this technique tends to over-estimate the toughness of  $Al_2O_3/Ag$  composites. In the present study, the toughness of the  $Al_2O_3/Ag$  composites is determined by the single-edge-notched-beam (SENB) technique. Furthermore, the effect of silver inclusions on the strength of alumina is not determined in the previous studies. In this study, the strength of the  $Al_2O_3/Ag$  composites is also measured.

## 2 Experimental Procedures

Alumina (AKP-50, Sumitomo Chem. Co. Ltd., Japan) and various amounts of silver oxide ( $Ag_2O$ , Johnson Matthey Co., UK) were milled in ethyl alcohol for 4 h. The slurry of the powder mixtures was dried with a rotary evaporator. The dried lumps were crushed and sieved. The powder compacts were prepared by pressing uniaxially at 56 MPa. The sintering was performed in air at 1600°C or 1700°C for 1 h. The heating and cooling rates were 5°C/min. In order to determine the toughness of alumina as a function of grain size, the alumina specimens with different grain size were prepared by sintering the alumina compacts at 1400–1700°C for 1 h. These  $Al_2O_3$  specimens

\*To whom correspondence should be addressed.

were prepared with the same procedures as those for the  $\text{Al}_2\text{O}_3/\text{Ag}$  composites.

The decomposition behaviour of silver oxide was determined by a differential thermal analyzer (DTA, Netsch Co., Germany). Phase identification was performed by X-ray diffractometry (XRD). The final density was determined by the water displacement method. Before submerging the specimens in water, a wax was applied to the surface to prevent water penetration. The microstructure was observed by a scanning electron microscope (SEM) and a transmission electron microscope (TEM). Both microscopes were equipped with an energy dispersive X-ray spectrometer (EDX). Polished surfaces were prepared by grinding and polishing with diamond paste to  $6\ \mu\text{m}$  and subsequently with silica suspension to  $0.05\ \mu\text{m}$ . Since the partial pressure of liquid silver at elevated temperature is high ( $10\ \text{mmHg}/1600^\circ\text{C}$  and  $23\ \text{mmHg}/1700^\circ\text{C}$ ),<sup>14</sup> a silver-free surface layer is formed.<sup>13</sup> After removing the silver-free layer by grinding, the volume fraction of silver after sintering was recalculated by counting the point fraction on the polished surfaces. The size of silver inclusions was determined by using the linear intercept technique. The dihedral angle of the silver inclusion within alumina matrix was estimated from polished microstructures by applying a stereological counting technique.<sup>15</sup> The polished specimens were thermally etched at  $1500^\circ\text{C}$  for 1 h to reveal the grain boundaries of alumina. The size of the matrix grains was also determined by the linear intercept technique. More than 200 grains or inclusions were counted.

The sintered specimens were machined longitudinally with a 325 grit resin-bonded diamond wheel at cutting depths of  $5\ \mu\text{m}/\text{pass}$ . The silver-free layer was removed during the grinding procedure. The final dimensions of the samples were  $3\ \text{mm} \times 4\ \text{mm} \times 36\ \text{mm}$ . The strength of the samples was determined by the 4-point bending technique at ambient conditions. The upper and lower spans

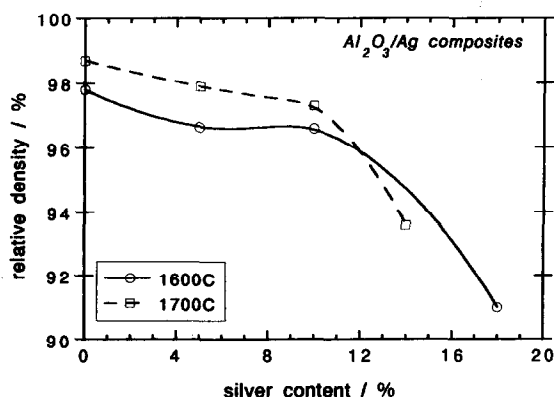


Fig. 1. The density of the composites as a function of silver content with the samples sintered at the indicated temperatures for 1 h.

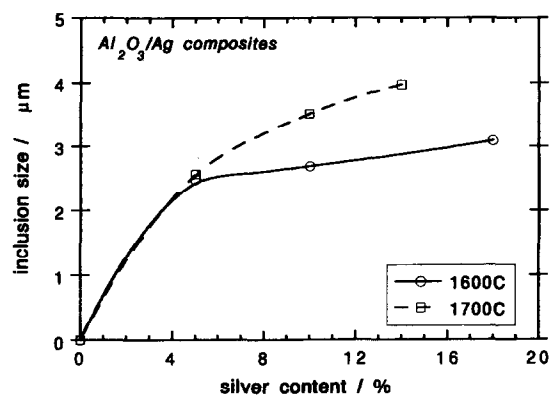


Fig. 2. The size of silver inclusions found in the composites shown in Fig. 1.

were 10 and 30 mm, respectively. The rate of loading was  $0.5\ \text{mm}/\text{min}$ . The fracture toughness was determined by the single-edge-notched-beam (SENB) technique. The notch was generated by cutting with a diamond saw. The width of the notch was around  $0.5\ \text{mm}$ . The indentation technique was also used to determine the toughness of the composites. The load applied was 50 N.

### 3 Results and Discussion

The DTA analysis suggests that the silver oxide starts to decompose from  $410^\circ\text{C}$ . The XRD patterns indicate that there is no residual silver oxide in  $\text{Al}_2\text{O}_3/\text{Ag}$  composites after sintering. The relative density of the composites is shown as a function of silver content in Fig. 1. The size of silver inclusions is shown as a function of silver content in Fig. 2. The grain size of alumina matrix is shown in Fig. 3. Typical microstructures for the composites are shown in Fig. 4. The dihedral angle of the silver inclusion within the alumina matrix is  $110 \pm 7.8^\circ$  for the composites sintered at  $1600^\circ\text{C}$  and  $101 \pm 5.5^\circ$  for the composites sintered at

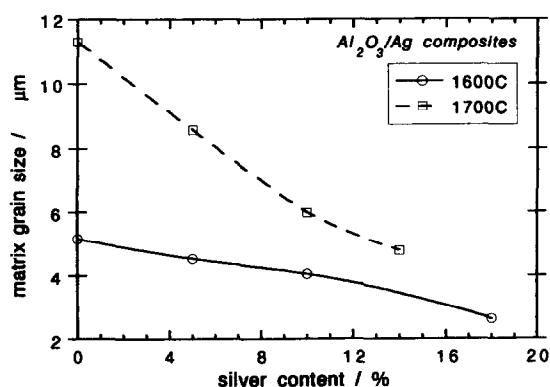


Fig. 3. The size of alumina matrix found in the composites shown in Fig. 1.

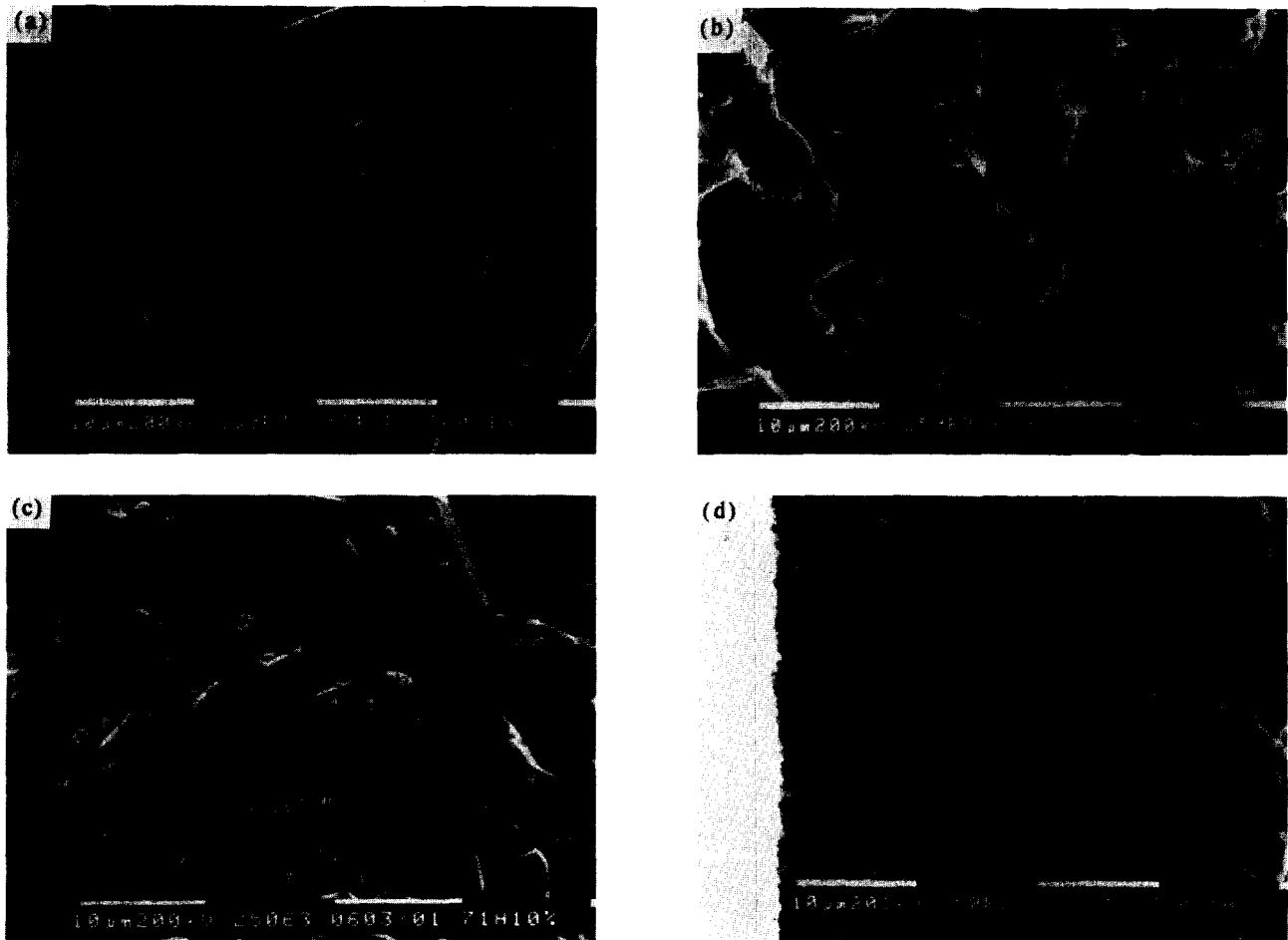


Fig. 4. Typical microstructures of  $\text{Al}_2\text{O}_3/\text{Ag}$  composites. The vol.% of silver in the composites shown is (a) 0, (b) 5, (c) 10 and (d) 14. The composites are sintered at  $1700^\circ\text{C}$  for 1 h.

$1700^\circ\text{C}$ . These values are close to the reported values determined by the sessile drop technique.<sup>16</sup> Since the wetting is poor, silver melt behaves as an inclusion to the alumina matrix. The densification of the alumina matrix is thus hindered. From Fig. 4, most silver inclusions are located at the grain boundaries of alumina, the grain growth of alumina matrix is slowed down due to the presence of silver inclusions.

Since the thermal expansion of silver (22/MK) is bigger than that of alumina (9/MK), thermal stress results after the cooling step. Twins can be observed within the silver inclusions, (Fig. 5). Due to the fact that the twins are lens-shaped, they are deformation twins.<sup>17</sup> It suggests that the silver inclusions are highly constrained due to the presence of residual stress. Occasionally, small particles can be observed near the  $\text{Al}_2\text{O}_3/\text{Ag}$  interface, (Fig. 5). The small particles analyzed by EDX are mainly composed of Cr and Fe. It may be from the contamination from the steel mold used for forming. From the TEM study, no reaction layer can be observed at the interface and no Al detected within the silver inclusions. Since the solubility of alumina in Ag is negligible, it further confirms that the silver melt can not act as an effective liquid

phase to promote the densification.

The fracture toughness of the composites is shown as a function of silver content in Fig. 6. The interactions between a crack and silver inclusions are shown in Fig. 7. In the figure, the crack is bridged by, or deflected by, the silver inclusions. It suggests that the toughening mechanisms for the composites are plastic deformation and crack deflection. Both the plastic deformation<sup>9-11</sup> and crack deflection<sup>18</sup> mechanisms can contribute to the toughness enhancement. The toughness of  $\text{Al}_2\text{O}_3/\text{Ag}$  composites determined by the SENB and indentation techniques is thus higher than that of  $\text{Al}_2\text{O}_3$  alone. However, the toughness determined by the indentation technique results in higher values. The crack opening introduced by the indentation is much smaller than the notch width produced by cutting with a diamond saw. Since the crack surfaces with a small opening are bridged by silver inclusions (Fig. 7), the propagation of the crack with a small opening is more difficult. Therefore, the toughness determined by the indentation technique is much higher than that determined by the SENB technique.

In order to determine the toughness of alumina matrix,  $K_{\text{IC,matrix}}$ , the toughness of the alumina



Fig. 5. A highly constrained silver inclusion found within the alumina matrix.

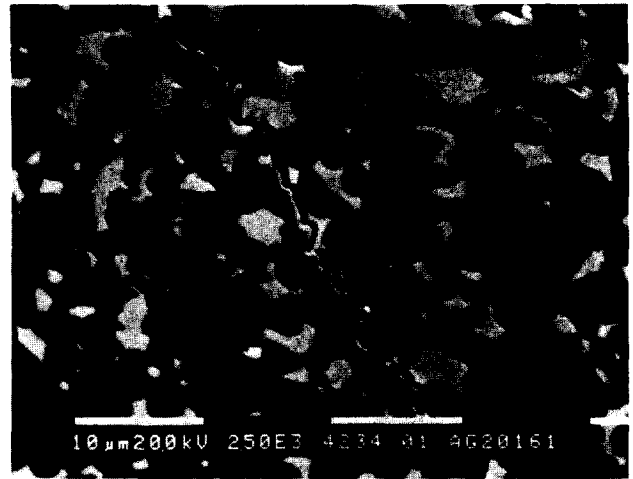


Fig. 7. The interactions between silver inclusions and a crack introduced by indentation.

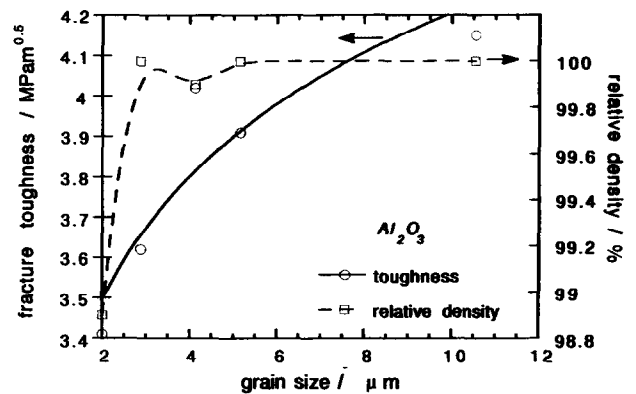


Fig. 8. The fracture toughness determined by the SENB technique and the density of  $\text{Al}_2\text{O}_3$  specimens as a function of grain size.

specimens sintered at various temperatures is determined (Fig. 8). The toughness is determined by the SENB technique. The density of the  $\text{Al}_2\text{O}_3$  specimens is varied from 98.9 to 99.9%; therefore, the effect of porosity on the toughness can be ignored. The toughness of alumina is increased with the increase of grain size. It is similar to the

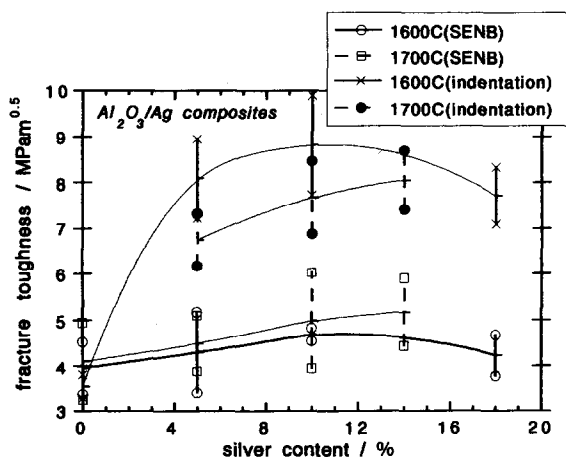


Fig. 6. The fracture toughness determined by the SENB and the indentation techniques for the composites shown in Fig. 1 as a function of silver content.

results reported by Tuan *et al.*<sup>19</sup> According to eqn (1), the toughness increase,  $\Delta K_{\text{IC,metal}}$ , contributed by the metallic inclusions which can be determined as  $K_{\text{IC,matrix}}$  is known. The toughness increase of the composites is shown as a function of the square root of the product of volume fraction,  $F$ , and inclusion size,  $d$ , in Fig. 9. Since the enhancement from the deflection around spherical inclusions is limited,<sup>18</sup> more significance is to be given to the

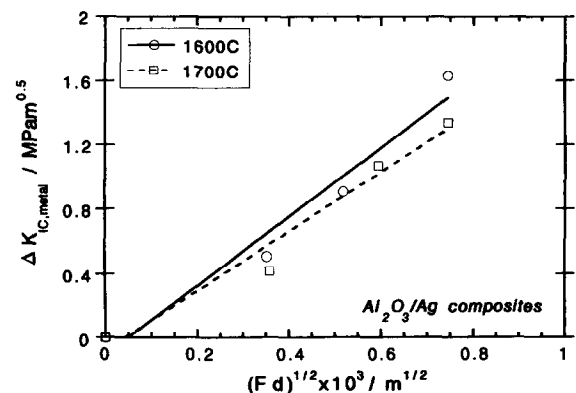


Fig. 9. The fracture toughness increase as a function of the square root of the product of volume fraction and inclusion size. The sintering temperatures are indicated.

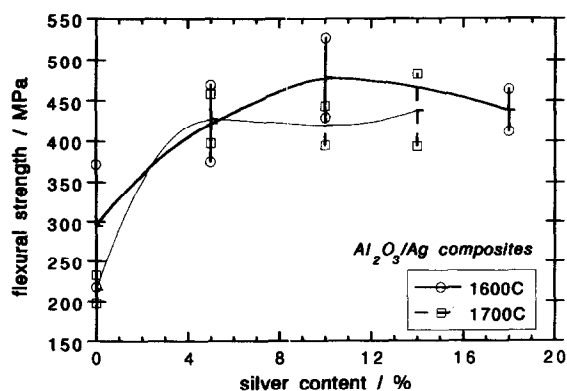


Fig. 10. The flexural strength for the composites shown in Fig. 1 as a function of silver content.

plastic deformation mechanism. This is supported by the linear relationship between the toughness increase and the square root of the product of volume fraction and inclusion size (Fig. 9).

The flexural strength of the composites is shown as a function of silver content in Fig. 10. With the enhanced toughness and the reduced grain size of alumina matrix as silver is added, the strength of alumina is improved substantially.

#### 4 Conclusions

Dense  $\text{Al}_2\text{O}_3/\text{Ag}$  composites are prepared by pressureless sintering at 1600°C and 1700°C for 1 h. The densification behaviour, microstructure development, and mechanical properties of the composites are investigated. Even though the silver inclusions are melted during sintering, due to the fact that the wetting of silver melt on alumina is poor and the solubility of alumina in silver is limited, the presence of silver inclusions hinders the densification. The matrix alumina grains are refined due to the grain boundaries being dragged by the silver inclusions. The addition of ductile inclusions not only toughens but also strengthens the ceramic matrix. The toughening is contributed mainly by the plastic deformation of silver inclusions. Due to the increase in toughness and the refinement of matrix grain size induced by the presence of the inclusions, the strength of the alumina is also significantly increased.

#### Acknowledgements

The present study is supported by the National Science Council, ROC., through the contract no.

NSC81-0405-E002-26. We are grateful for the valuable comments given by Prof. R. J. Brook, Oxford University.

#### References

- Rankin, D. T., Stiglich, J. T., Petrak, D. R. & Ruh, R., Hot-pressing and mechanical properties of  $\text{Al}_2\text{O}_3$  with Mo-dispersed. *J. Am. Ceram. Soc.*, **54** (1971) 277.
- Flinn, B. D., Ruhle, M. & Evans, A. G., Toughening in composite of  $\text{Al}_2\text{O}_3$  reinforced with Al. *Acta Metall.*, **37** (1989) 3001.
- Baran, G., Degrangé, M., Rouques-Carmes, C. & Wehbi, D. Fracture toughness of metal reinforced glass composite. *J. Mater. Sci.*, **25** (1990) 4211.
- Aghajanian, M. K., Macmillan, N. H., Kennedy, C. R., Luszcz, S. J. & Roy, R., Properties and microstructures of Lanxide  $\text{Al}_2\text{O}_3\text{-Al}$  ceramic composite materials. *J. Mater. Sci.*, **24** (1989) 658.
- Wu, S., Gesing, A. J., Travitzky, N. A. & Claussen, N., Fabrication and properties of Al-infiltrated RBAO-based composites. *J. European Ceram. Soc.*, **7** (1991) 277.
- Tuan, W. H. & Brook, R. J., The toughening of alumina with nickel inclusions, *J. European Ceram. Soc.*, **6** (1990) 31.
- Tuan, W. H. & Wu, J. M., Effect of microstructure on the hardness and toughness of  $\text{YBa}_2\text{Cu}_3\text{O}_{7-x}/\text{Ag}$  composites. *J. Mater. Sci.*, **28** (1993) 1415.
- Becher, P. F. & Tiegs, T. N., Toughening behaviour involving multiple mechanisms: whisker reinforcement and zirconia toughening. *J. Am. Ceram. Soc.*, **70** (1987) 651.
- Ashby, M. F., Blunt F. J. Bannister, M., Flow characteristics of highly constrained metal wires. *Acta Metall.*, **37** (1987) 1847.
- Bannister, M. & Ashby, M. F., The deformation and fracture of constrained metal sheets. *Acta Metall.* **39** (1991) 2575.
- Deve, H. E., Evans, A. G., Odette, G. R., Mehrabian, R., Emiliani, M. L. & Hecht, R. J., Ductile reinforcement toughening of  $\gamma\text{-TiAl}$ : effects of debonding and ductility. *Acta Metall.*, **38** (1990) 1491.
- Tuan, W. H. & Chou, W. B., Toughening alumina with silver inclusions, *Proc. of the 2nd European Ceram. Soc.*, Vol. 2, ed. by Ziegler, G. & Hausner, H., Vol. 2, Deutsche Kermische Gesellschaft e.V., Germany 1991, pp. 1703.
- Wang, J., Ponton, C. B. & Marquis, P. M., Silver toughened alumina ceramics. *Br. Ceram. Trans.*, **92** (1993) 67.
- Wise, E. M. & Coxe, C. D., in *Metal Handbook*, Vol. 1, Am. Soc. for Metal, Ohio, USA, 1961, pp. 1181.
- DeHoff, R. T., Estimation of dihedral angles from stereological counting measurements. *Metallography*, **19** (1990) 209.
- Nikolopoulos, P. & Agathopoulos, S., Interfacial phenomena in  $\text{Al}_2\text{O}_3\text{-liquid metal}$  and  $\text{Al}_2\text{O}_3\text{-liquid alloy}$  systems. *J. European Ceram. Soc.*, **10** (1992) 415.
- Wang, J., Ponton, C. B., Marquis, P. M., The microstructure of pressureless sintered silver-toughened alumina: an in-situ TEM study. *Mater. Sci. Eng.*, **A161** (1993) 119.
- Faber, K. T. & Evans, A. G., Crack deflection processes — I. Theory. *Acta Metall.*, **31** (1983) 565.
- Tuan, W. H., Lai, M. J., Lin, M. C., Chan, C. C. & Chiu, S. C., The mechanical performance of alumina as a function of grain size. *Mater. Chem. Phys.*, **36** (1994) 246.